

**The Hydrometeorology of a Deforested Region of the Amazon Basin**

RENATO RAMOS DA SILVA AND RONI AVISSAR\*

Department of Civil and Environmental Engineering, Duke University, Durham, NC

(Manuscript received 21 March 2005, in final form January 2006)

ABSTRACT

A series of numerical simulations were performed to evaluate the capability of the Regional Atmospheric Modeling System (RAMS) to simulate the evolution of convection in a partly deforested region of the Amazon basin during the rainy season, and to elucidate some of the complex land-atmosphere interactions taking place in that region. Overall, we demonstrate that RAMS can simulate properly the domain-average accumulated rainfall in Rondônia when provided with reliable initial profiles of atmospheric relative humidity and soil moisture. It is also capable of simulating important feedbacks involving the energy partition at the ground surface and the formation of convection. In general, more water in the soil and/or the atmosphere produces more rainfall. But these conditions affect the onset of rainfall in opposite ways; while higher atmospheric relative humidity leads to early rainfall, higher soil moisture delays its formation. As compared to stratiform clouds, which tend to cover a large area, convective clouds are localized and they let relatively more solar radiation reach the ground surface. As a result, a stronger sensible heat flux is released at the ground surface, which enhances the atmospheric instability and reinforces convection. Simulations using horizontal grid elements 2 and 4 km in size show a delay and decrease of rainfall as compared to simulations with high-resolution grids whose elements are not larger than 1 km and, as a result, afflict RAMS performance. We conclude that RAMS can be used as a reliable tool to simulate the various hydrometeorological processes involved in land-cover changes as a result of deforestation in this region.

-----  
**1. Introduction**

Amazonia is a hydrographic basin of great hydrologic importance. It covers an area of 6 million km<sup>2</sup> of tropical forest (Goulding et al. 2003), receiving a total average rainfall of 2500 mm per year (Richey et al. 1991), generating an annual

discharge of over a trillion cubic meters of water into the Atlantic Ocean (Vital and Statterger 2000). Recent human activity in the area has caused a gross rate of deforestation on the order of 18000 km<sup>2</sup> yr<sup>-1</sup> (INPE 2002). The hydroclimatic changes resulting from this replacement of natural

---

\* *Corresponding author address:* Dr Roni Avissar, Department of Civil and Environmental Engineering, Duke University, 123 Hudson Hall, PO Box 90287, Durham, NC, 27708-0287; Tel: 919 660-5458, Fax: 919 660-5459; E-mail: avissar@duke.edu

forest by degraded vegetation has yet to be fully understood and quantified; estimating its impact is very important not only for the region but also for the global water cycle (Avisar and Nobre 2002; Avisar and Werth 2005).

Data analysis show that most of the moisture into the Amazon River basin comes from the Tropical Atlantic (Rao et al. 1996). Also, long-term observations suggest that the convergence of moisture over the region has increased in the last 40 years, producing more precipitation mainly during the rainy season (Henderson-Sellers et al. 2002). Two possible reasons have been suggested for this increase of rainfall: greenhouse gas-induced hydroclimate change or locally-induced increase of convection (Henderson-Sellers and Pitman 2002).

Governmental projects for the development of the Amazon (such as the one in Rondônia) have resulted in a patchy landscape of forest and pasture that has a characteristic length scale of about 4 km (Calvet et al. 1997). Satellite observations show an increase of cloudiness at the boundary of these patches during the dry season (Cutrim et al. 1995; Negri et al. 2004) and the rainy season (Durieux et al. 2003). The possible effects of land-cover change on convective clouds during the rainy season are still not well understood.

The impacts of land-cover change on rainfall may evolve in different ways. A massive deforestation is likely to reduce rainfall due to a decrease in the transpiration and surface roughness and an increase in albedo as has been shown in various studies with general circulation models (GCMs). The current level of deforestation, however, may create mesoscale circulations that could enhance convection and promote a transient increase of rainfall (Avisar et al. 2002).

To better understand the hydrometeorological processes involved in

this region, an intensive observation campaign was carried out in the rainy season between January and February of 1999 as part of the Large Scale Biosphere-Atmosphere Experiment in Amazonia (LBA) (Avisar and Nobre 2002). A large number of meteorological observations with radars, radiosondes, micrometeorological towers, rain gauges, weather stations, and airplanes were collected during this field study in Rondônia, which is referred to as the “Wet Atmospheric Mesoscale Campaign (WetAMC)”. These observations show that the wind regime and the landscape (i.e., land cover and topography) have important impacts on convection and precipitation (Halverson et al. 2002). But even when carried out extensively, observations alone are not sufficient to explain all the processes involved in this complex hydrometeorological system. Indeed, most measurements are made only at a few locations for limited periods, and often lack temporal and spatial resolution. In addition, instruments measure only a small number of variables, which are not sufficient to explain all the physical, biological and chemical mechanisms and feedbacks involved in these processes. State-of-the-art models are useful tools to bridge the gap in our understanding.

Several studies have been conducted with global and regional numerical models. But experiments performed with GCMs use grid size in the order of 2-5 degrees of latitude and longitude (Nobre et al. 1991; Werth and Avisar 2002). At such coarse resolution, mesoscale circulations are not resolved, and while a few attempts have been made to develop an appropriate parameterization (Lynn et al. 1995, Liu et al. 1999, Donner et al. 2001) important issues remain to be solved and no GCM yet accounts for them through subgrid-scale parameterizations (Avisar et al. 2002). Current GCMs subgrid-scale parameterizations represent convection and microphysical cloud

processes based on the large-scale mean state of the atmosphere, which leads to errors in rainfall modeling (Molinari and Dudek 1992).

So far, it has not been shown that atmospheric models are capable of simulating realistically precipitation during the wet season in the Amazon. Indeed, they tend to produce too early rainfall in Rondônia (Betts and Jakob 2002), and too high precipitation east of the Andes (Horel et al. 1994; Tanajura 1996; Chou et al. 2000; Chou et al. 2002; Druyan et al. 2002; Misra et al. 2002). Roads et al. (2003) performed an inter-comparison of several models applied to this region and concluded that they are overly dry over much of the domain as compared to observations. The errors seem to be associated with the models' convective parameterization. Currently, the only known method to avoid this problem is by performing high-resolution simulations. Thus, a careful evaluation of the capability of the models to represent weather events associated with moist convection in the Amazon is necessary as a first step to achieve better long-term regional simulations (Takle et al. 1999).

Several studies have been performed with mesoscale models to understand the effects of land-cover change on the dynamics of local circulations and convection in the Amazon (Silva Dias and Regnier 1996; Souza et al. 2000; Wang et al. 2000; Baidya Roy and Avissar 2002; Silva Dias et al. 2002). These numerical studies provided important preliminary understanding of the convection dynamics in that region. However, the majority of these studies focused on the dry season, and/or were limited to only a few cases. Furthermore, the models used have not been carefully evaluated, partly due to the scarcity of data. But, to use confidently a model to study precipitation in the Amazon basin a detailed evaluation of its capability to simulate the

hydrometeorological processes in that region during the rainy season remains to be demonstrated. Here, we show that modeling moist convection accurately in this region requires: (1) a reliable representation of the current landscape heterogeneity; (2) a grid mesh with elements not larger than 1 km to explicitly resolve convection; (3) a grid mesh that covers a large domain to correctly represent relevant mesoscale dynamical processes; (4) several case studies with various meteorological background conditions during the wet season to have a robust evaluation; and (5) a comparison with reliable observations.

The goal of the study summarized in this article is twofold: (1) evaluate the performance of a state-of-the-art numerical model based on recent observations collected during the LBA field campaign together with vegetation characteristics derived from modern satellites, and (2) improve our understanding of the effects of deforestation on the hydrometeorology of the Amazon basin. For that purpose, the model used here is set up to represent the landscape heterogeneity and convection at a very high resolution, it covers a large area, and it is compared with state-of-art observations collected during the LBA WetAMC.

## 2. Numerical Experiments

The Regional Atmospheric Modeling System (RAMS) (Pielke et al. 1992; Cotton et al. 2003) is used here together with observations collected during the LBA WetAMC in an area where deforestation has generated a patchy landscape of forest and pasture (see Fig. 1). RAMS is a three-dimensional model consisting of a set of prognostic equations, including dynamics, thermodynamics, and hydrometeor microphysics. These equations are solved numerically using finite difference schemes applied to a staggered Arakawa C-grid. The model contains several interacting sub-

models that simulate soil-vegetation-atmosphere exchange of heat and water (Avisar and Pielke 1989; Walko et al. 2000a); surface-layer turbulent processes (Louis 1979); boundary-layer turbulent processes (Mellor and Yamada 1974; Deardorff 1980); solar and thermal radiation transfer and its interaction with hydrometeors (Harrington 1997); and cloud microphysics and precipitation (Walko et al. 1995; Walko et al. 2000b). RAMS scored quite well in various evaluation studies, such as large-eddy simulations (Avisar et al. 1998), mesoscale systems (Silva Dias and Regnier 1996; Weaver and Avisar 2001; Baidya Roy and Avisar 2002; Nair et al. 2003), and regional climate (Takle et al. 1999; Liston and Pielke 2001; Gandu et al. 2004; Hasler et al. 2005).

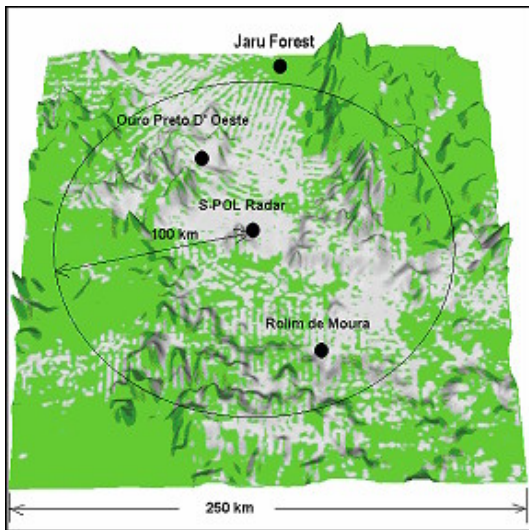


**FIG. 1.** Physiographical characteristics of the studied area in Rondônia (Brazil). Forest is green and deforested areas are white. This domain is centered at  $[11^{\circ}22'S, 62^{\circ}00'W]$  and covers the region in which most of the meteorological instruments were deployed during the LBA WetAMC. The circle represents the S-POL radar scanning area.

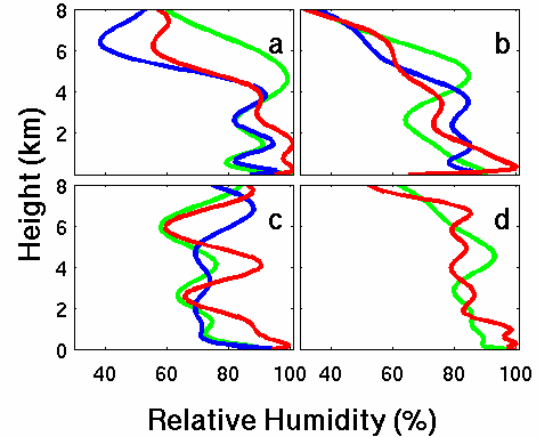


**FIG. 2.** Measured relative humidity profiles in Rondônia at the Jaru Forest (green), Ouro Preto D'Oeste (red) and Rolim de Moura (blue) (See Fig. 1 for locations) at 0800 LT (1200 UTC) on (a) 04 February, (b) 06 February, (c) 14 February, and (d) 23 February. A polynomial function was used to extrapolate between observation points.

The cloud microphysics package in RAMS is based on a set of prognostic equations for the prevailing hydrometeors (Walko et al. 1995; Meyers et al. 1997; Walko et al. 2000b). Water is partitioned in up to eight forms: vapor, cloud droplets, liquid rain, pristine ice, snow, aggregates, graupel and hail. Cloud droplets and rain are liquid water that may be super-cooled. Pristine ice, snow and aggregates are assumed to be completely frozen, while graupel and hail are mixed-phase categories, capable of comprising ice only or a mixture of ice and liquid. The model calculates the concentration of vapor in an atmospheric column and prognoses the formation of different hydrometeors. Their size distribution is determined using a two-moment statistical scheme (Meyers et al. 1997). The model also follows the exchange of water and energy as hydrometeors interact with vapor and between themselves (Walko et al. 2000b).

The domain simulated here consists of 250 by 250 horizontal grid elements, each representing a 1 km by 1 km area, centered at 11°22'S, 62°00'W in Rondônia, Brazil (Fig. 1). This domain was chosen for two reasons. First, it possesses the major features believed to have a significant impact on precipitation variability in Rondônia (i.e., topography and land-cover variability). Second, it covers the region in which most of the meteorological instruments were deployed during the LBA WetAMC including the S-band polarization (S-POL) radar that is located at its center. At a horizontal grid size of 1 km and a vertical grid size of about 100 meters in the boundary layer, RAMS resolves cumulus, thus avoiding the complications encountered in subgrid-scale parameterizations used in coarse-resolution models. Subgrid turbulence is parameterized with the Mellor-Yamada (1974) scheme.

In the vertical, the grid structure has higher resolution near the ground surface and is stretched with height, starting 30 m above ground and progressively increasing the grid elements up to a size of 1.5 km near the top of the domain, which is set at a height of 22.5 km.

Homogeneous initial conditions are assumed in all numerical experiments. Silva Dias et al. (2002) found that this initialization method is best suited for short simulations, and it is extensively used in convection-resolving models (Emanuel 1994, pg 307).

Figure 2 shows observed profiles of relative humidity (RH) at three locations in Rondônia at 0800 LT (i.e., 1200 UTC) for different days of the WetAMC. The model is initialized with homogeneous conditions using the atmospheric profiles retrieved from the radiosondes launched at Jaru Forest because it is available for all the studied cases and compares well with the sounding from Rolim de Moura. Lateral boundary

conditions are calculated following the approach proposed by Klemp and Wilhelmson (1978). With this approach, a normal velocity component is specified at the boundary (20 m/s in our case), which allows most disturbances to propagate outside the simulated domain without reflecting strongly towards the internal domain. We also explored using the global NCEP reanalysis data (Kalnay et al. 1996) to force the model at its lateral boundaries. However, probably due to its too coarse resolution (which is 2.5 degree) for the small domain simulated here, results were generally less good. Note that the profiles measured at Ouro Preto D'Oeste have a larger humidity in the boundary layer. Betts et al. (2002) identified and discussed this wet bias at this measurement site. RH profiles at Ouro Preto D'Oeste were corrected with the measurements collected in the atmospheric boundary layer (ABL) with a tethered balloon (Betts et al. 2002). At this location, the atmosphere is often saturated. Tests using saturated profiles as initial conditions in RAMS produce unrealistic immediate cloudiness over the entire domain, which reduce the amount of solar radiation reaching the surface and induce a negative land-atmosphere feedback that affects the development of the ABL. The average relative humidity in the first 1000 m of the atmosphere for February 4, 6, 14, and 23 (hereinafter F04, F06, F14 and F23) is 86%, 84%, 78%, and 90%, respectively, indicating that F04 and F23 were wetter than the other two days.

The integration time step of the model is 5 seconds and the simulated period is 12 hours for each case study, starting at 0800 LT. Thus, only the day-time evolution of the convective boundary layer is simulated.

The soil numerical grid is also stretched and consists of 12 layers, starting from the surface down to a depth of 4 meters, with a higher resolution near the surface. Dawson

(1993) and Nepstad et al. (1994) found that vegetation in the Amazon basin can uptake water from deep soil layers, thus requiring the grid selected here. Soil moisture is initialized homogeneously over the entire simulated domain based on a profile observed at Ouro Preto D'Oeste (Rondônia) during the WetAMC (Alvala et al. 2002). Accordingly, at the first level below the surface, the initial soil moisture was set to 39% of saturation, increasing linearly to 45% of saturation at the deepest layer. A sandy-clay-loam soil texture was assumed in accordance with the predominant soil observed in this region (Alvala et al. 2002).

To realistically represent the landscape of the region, vegetation characteristics estimated from Landsat satellite images by Calvet et al. (1997) were adopted for our simulations (Fig. 1). Two types of land covers were defined: evergreen forest (tropical forest) and short grass (pasture). To model these vegetation types, several parameters estimated from in situ measurements (Gash and Nobre 1997) and tested in recent numerical experiments (Gandu et al. 2004) were adopted. They are summarized in Table 1.

The four days selected to evaluate the model (F04, F06, F14, and F23) were characterized by local formation of convection under different synoptic-scale meteorological conditions. High-quality observations were recorded for these four days. Cases having propagation of large-scale convective systems into the domain of study were avoided because they would require an even larger simulation domain with too many grid points to be realistically simulated with readily available computing resources. Analysis of the S-POL radar reflectivity (NCAR 1999) shows that storms were propagating from the east on F04 and F14, from the west on F23 and were quasi-stationary (slight westward propagation) on F06. Corresponding total accumulated

rainfall obtained by integrating 10-minute rainfall rate estimates is presented in Figure 3. Light rainfall accumulated all over the domain and high rainfall accumulated near the western hills on F04, F06 and F14. On F23, rainfall accumulated more in the southeast region of the domain. These accumulations seem to be associated with the large-scale winds in the free-atmosphere that are responsible for the storms propagation.

TABLE 1. Vegetation parameters used in RAMS to characterize “forest” and “pasture” in the Amazon basin.

Parameter	Forest	Pasture
Albedo	.13	.18
Emissivity	.95	.96
Leaf Area Index	5.0	2.0
Vegetation Fraction	.98	.80
Roughness Length (m)	2.0	.02
Displacement Height (m)	20.0	.2
Root Depth (m)	4.0	1.0
Maximum Stomatal Conductance ( $\text{ms}^{-1}$ )	.0035	.01

The model set-up described in this section is assumed to be the control run for each case study and is used to evaluate the model performance against the observations. Modeling convection is highly sensitive to initial conditions (Lorenz 1963). Therefore, in addition to the control simulations, a few sensitivity tests are performed using various initial conditions, especially for those estimated with a lack of a high level of confidence (e.g., soil moisture and relative humidity).

Coarse-grid simulations have the advantage of low computational cost. While a few numerical experiments have been performed to simulate the rainy season in Rondônia at different grid resolutions (Wang et al. 2000; Silva Dias et al. 2002), a careful evaluation of model performance as a function of grid resolution has not yet

conducted. This issue is explored here using grid sizes of 2, 4 and 20 km in addition to the control simulations that use a 1-km grid mesh.

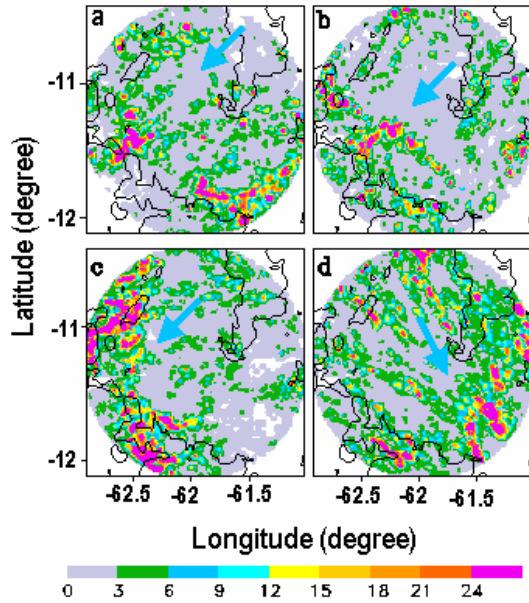


**FIG. 3.** Accumulated precipitation (mm) derived from the S-POL radar between 0800 LT and 2000 LT on (a) 04 February, (b) 06 February, (c) 14 February and (d) 23 February. The blue arrows represent the horizontal wind used to initialize the model above the atmospheric boundary layer (at a height of 1642 m). Contour lines represent topography higher than 300 m.

### 3. Results

#### a. Control simulation

Figure 4 presents the spatial distribution of accumulated precipitation for the control simulation of each one of the four case studies. Only the inner 200 km domain is displayed for a clearer comparison with the radar estimates shown in Fig. 3. The wind directions at two heights emphasize the various meteorological conditions prevailing during the rainy season in Rondônia. There is no good spatial correlation between the simulated and S-POL radar-derived rainfall

estimates but their comparison shows similar structure during the onset stage of precipitation caused by topographic forcing. These differences can be partly explained by the inaccuracy of initial and boundary conditions in the simulations. But it is very important to keep in mind that convection is chaotic in nature and, therefore, the timing and location of a precipitation cell cannot be expected to be exactly similar in the model and the observations. Only their statistical properties are comparable. Furthermore, in the tropics, mesoscale systems are mostly triggered by local convection, which has a characteristic size of the order of 2-20 km (i.e., meso- $\gamma$  scale) and a very large Rossby radius of deformation. Therefore, their predictability is considerably lower than at mid-latitudes, where meso- $\alpha$  systems that are more baroclinic and are shaped by geostrophic winds, dominate.

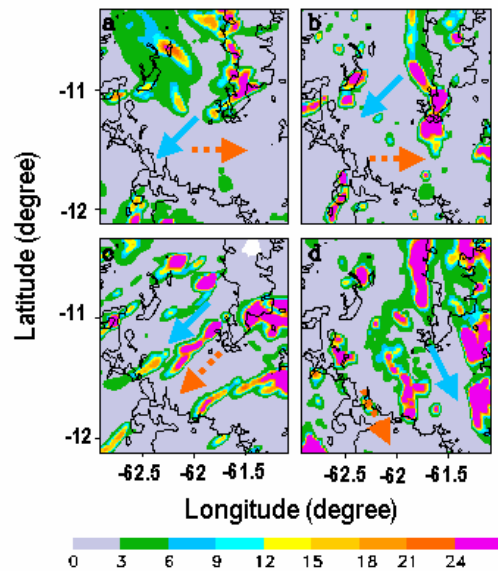


**FIG. 4.** Same as Fig. 3 but for the simulated precipitation with RAMS. The additional orange arrows are for the initial wind at 314 m.

Figure 5 shows the domain-average, accumulated rainfall simulated with RAMS

as compared to corresponding estimates from the S-POL radar. Averages are computed for the region encircling the radar location, with a radius of 100 km (see Fig. 1). The control simulations produce accumulated rainfall very similar to the radar estimates. Correlation coefficients between model results and observations are .98, .98, .95 and .98 for F04, F06, F14, and F23, respectively. In general, the onset of rainfall in the model is delayed as compared to that observed with the radar. Later in the afternoon, the simulated rainfall is stronger than that seen by the radar, and this compensates for the late onset of the simulated precipitation.

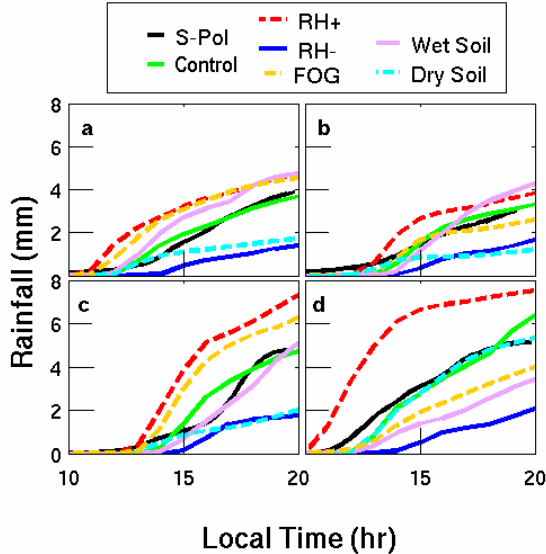


**FIG. 5.** Domain-average accumulated precipitation simulated with RAMS and estimated from the S-POL radar on (a) 04 February, (b) 06 February, (c) 14 February and (d) 23 February.

Figure 6 shows the frequency of grid elements of accumulated rainfall obtained from the simulations and from the radar. For a more appropriate comparison between them, the model results that were obtained on a 1 x 1 km grid were regridded into a 2-km data set. Although there are discrepancies in regions receiving light and heavy

accumulation of rainfall, the simulations and the radar provide similar results over the domain, when precipitation is within the 3 - 30 mm range. At several locations, the radar does not detect any precipitation, while the model produces light accumulation.

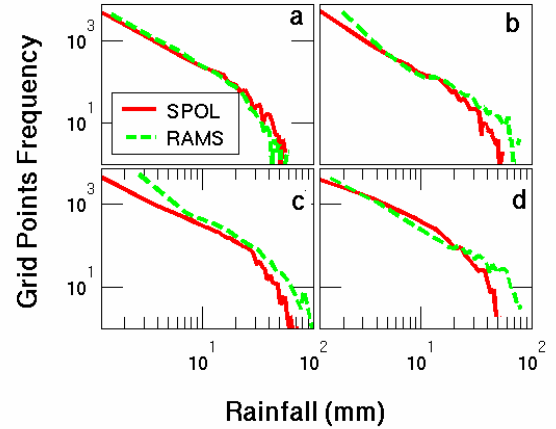


**FIG. 6.** Frequency distribution of accumulated rainfall between 0800 and 2000 LT on (a) 04 February, (b) 06 February, (c) 14 February and (d) 23 February.

The S-POL radar is based on the polarimetric method that is sensitive to raindrop deformation to estimate the rainfall rate. This method is not sensitive to small droplets and, therefore, this radar does not provide a reliable estimate of light rainfall. Also, RAMS produces heavy accumulation at several locations that is not captured by the radar. Comparing radar data with raingauge observations during the WetAMC, Carey et al. (2000) showed that the radar under-estimates events of high rainfall rate. Furthermore, RAMS, like any other model, is based on various approximations and it is unlikely to simulate perfectly the real precipitation. Table 2 indicates that, in general, RAMS simulates well not only the mean accumulation but also its median, tri-mean, median absolute deviation (MAD) and inter-quartile range (IQR). But on F14, the discrepancies in light rainfall are also reflected in these other

statistical properties. In this case the model produces high rainfall accumulations over small areas while the radar shows weak rainfall distributed over large areas. Nevertheless, similar means are obtained with both methods (Tables 2 and 3).

TABLE 2. Simulated (with RAMS) and S-POL-radar-derived statistical moments of rainfall total accumulation at 2000 LT.

		S-POL	RAMS
F04	Mean	3.9	3.7
	Median	1.2	1.4
	Tri-mean	2.0	2.2
	MAD	1.1	1.0
	IQR	3.8	3.4
F06	Mean	3.1	3.3
	Median	0.5	0.5
	Tri-mean	1.3	1.0
	MAD	0.5	0.3
	IQR	2.7	1.4
F14	Mean	4.8	4.7
	Median	1.4	0.9
	Tri-mean	2.9	1.9
	MAD	1.4	0.7
	IQR	6.0	3.0
F23	Mean	5.9	6.4
	Median	2.4	1.9
	Tri-mean	3.4	3.0
	MAD	2.0	1.1
	IQR	5.8	4.1

Figures 7 and 8 show the simulated vertical profiles of predominant wind direction and domain-average wind speed, as compared to observations at 1700 LT. The predominant wind is assumed to be that wind whose direction is the most frequent at a given atmospheric level. RAMS simulates well this variable in most cases, but there are a few discrepancies that may affect the spatial distribution of rainfall. For example, on F04 (Fig. 7a), the observed winds are from the northeast in the layer between 1 and 3 km, while the model predominant

wind is from the southeast. On F14 (Fig. 7c), in the layer between 2 and 4 km, observed winds are from the east, while the simulated predominant wind is from the northeast. These discrepancies may be due to the use of homogeneous initial conditions and the lack of large-scale atmospheric gradients that possibly exist over the simulated domain but are not accounted for properly with the homogeneous forcing used in our numerical experiments. Furthermore, the observations are instantaneous values at the given sites, while the modeled winds are spatially averaged over the entire domain and time step. Thus, they are not strictly similar.

Using radar and satellite data, Laurent et al. (2002) showed that storms propagate along with mid-level winds. Weisman and Klemm (1986) concluded that, in general, weak wind shear is associated with individual convective cells, while strong shear induces multi-cell convective systems. Thus, a misrepresentation of the wind shear may affect the storm evolution and the spatial distribution of rainfall, as discussed in detail in Section 3.e.

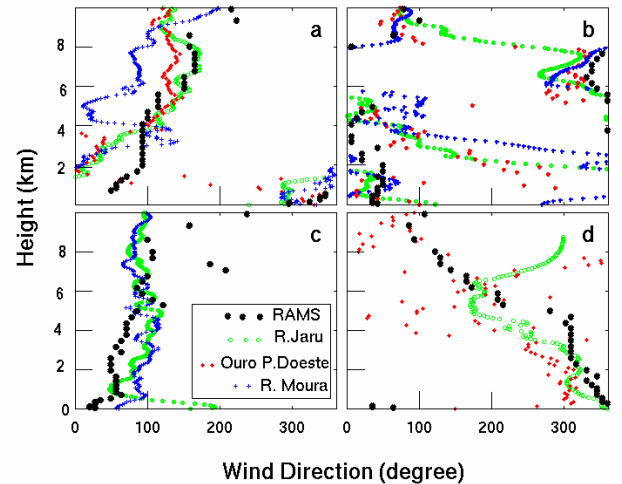
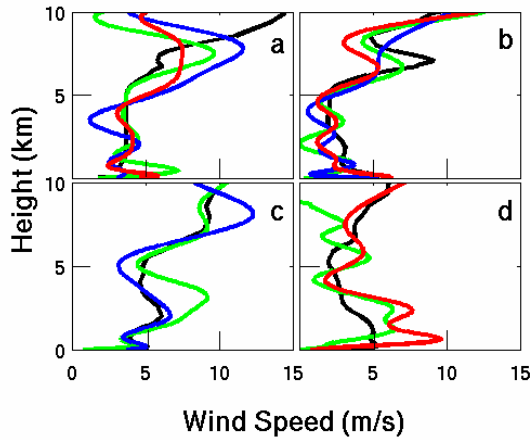


FIG. 7. Simulated predominant wind direction as compared to observations at 1700 LT on (a) 04 February, (b) 06 February, (c) 14 February, and (d) 23 February. The predominant wind at each atmospheric level is defined as the most frequent direction at that level.

TABLE 3. Simulated rainfall area (km<sup>2</sup>), domain-average rainfall (mm) for locations with precipitation greater than 1mm, and maximum accumulated precipitation (mm) obtained at 2000 LT.

		S-POL	Cntrl	RH+10%	RH-10%	WetSoil	DrySoil	Fog
F04	Area	16592	18980	24776	9276	15984	12384	22764
	Rainfall	7.07	5.68	5.75	3.89	8.79	3.54	5.98
	Max	67.38	67.55	60.10	38.57	100.2	36.56	54.47
F06	Area	12760	9840	15740	5684	8684	6856	10632
	Rainfall	6.91	9.74	7.03	8.53	14.59	4.84	8.50
	Max	52.89	78.23	112.7	53.36	95.33	46.39	95.28
F14	Area	17300	14320	24112	5592	13732	16712	18164
	Rainfall	9.05	9.76	9.26	8.95	11.18	3.20	10.32
	Max	73.94	149.9	160.7	61.97	128.0	22.50	202.09
F23	Area	21708	23496	25296	9608	25204	17568	22240
	Rainfall	7.23	8.18	9.13	5.80	4.01	9.10	4.72
	Max	72.99	79.98	96.77	65.90	65.80	85.29	57.29



**FIG. 8.** Simulated domain-average wind speed profiles (black) as compared to observations at 1700 LT on (a) 04 February, (b) 06 February, (c) 14 February, and (d) 23 February. Observations are from Jaru Forest (green), Rolim de Moura (blue), and Ouro Preto D'Oeste (red). A polynomial function was used to extrapolate between observation points.

#### *b. Sensitivity to Initial Atmospheric Moisture*

Betts et al. (2002) emphasized that atmospheric moisture is highly susceptible to measurement errors, especially in the

tropics. Therefore, evaluating the potential impact of biased initialization of atmospheric moisture on the simulated rainfall is important. Here, this was achieved by raising the model's initial relative humidity profile by 10% in one case and decreasing it by the same amount in another case. As it can be seen in Fig. 5, higher initial atmospheric moisture results in earlier and larger accumulation of rainfall in all cases. It is interesting to note that this higher atmospheric moisture produces about 50% more rainfall on F14, and rainfall starts about 1-2 hours earlier than in the control case. Overall, higher initial atmospheric moisture results in stronger storms, with more rainfall that covers larger areas (Table 3). By contrast, decreasing the model's initial relative humidity by 10% results in reduced and delayed rainfall. Thus, misrepresenting the initial moisture profile, such as the possible wet bias observed in Ouro Preto D'Oeste, leads to large errors in modeling the amount and timing of rainfall.

Early-morning, low-level clouds (i.e., fog) are commonly observed in the region. Their formation is due to the cool, moist conditions near the surface at this time of the day. Imposing an initial profile of relative

humidity at saturation in the boundary layer only (namely the lowest 500 meters of the atmosphere) generates low-level clouds almost immediately in RAMS. Such fogs also affect the timing of precipitation and its accumulation (Fig. 5). Interestingly, in some cases, morning fogs increase rainfall accumulation (F4 and F14) while in others, they decrease it (F06 and F23), revealing complex interactions between the surface, clouds, and rainfall in this wet environment.

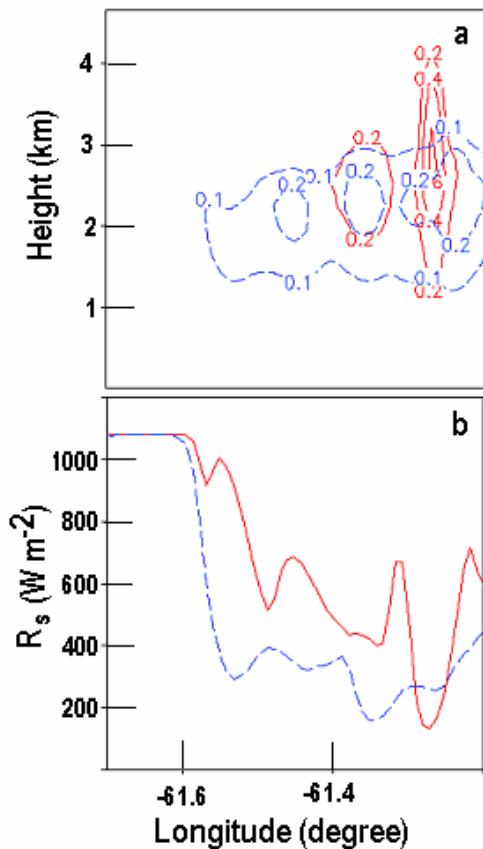


**FIG. 9.** Simulated vertical, west-east cross section of (a) rainfall ( $\text{g kg}^{-1}$ ), and (b) downward solar radiation at the surface,  $R_s$ , at latitude  $10.8^\circ\text{S}$  at 1200 LT on 23 February, resulting from the initialization of a dry soil (continuous line) and wet soil (dashed line).

### c. Sensitivity to Initial Soil Moisture Content

Initial soil moisture is known to have a strong effect on the modeling of

precipitation (Chang and Wetzel 1991; Beljaars et al. 1993; Pielke et al. 1997). Due to its significant impact on evapotranspiration and soil thermal properties, one can speculate that it has a significant impact on hydrometeorological conditions in the Amazon basin as well. Here, we check its impact by increasing it by 15% over the entire domain in one case and decreasing it by the same amount in another.

Similar to the higher relative humidity case discussed previously, a wetter soil produces more rainfall, except on F23 (Fig. 5d and Table 3). In that case, the combination of high moisture in the soil and the atmosphere creates stratiform clouds and rain, in contrast to the convective type obtained with the dry soil. This is illustrated in Fig. 9, which depicts a vertical cross section of cloud mixing ratio in the atmosphere above the hilly terrain of the northeastern part of the simulated domain. The narrow and deep convective cell has a rain mixing ratio greater than  $0.6 \text{ g kg}^{-1}$ , while the shallow, widely spread stratiform cloud only reaches a value of  $0.2 \text{ g kg}^{-1}$ . Figure 9 also shows that, at 1200 LT, the stratiform cloud reduces more significantly the solar radiation reaching the ground surface. The downward long-wave radiation is about  $460 \text{ W m}^{-2}$  for convective clouds and about  $440 \text{ W m}^{-2}$  for stratiform clouds, emphasizing a stronger effect of cloud type on solar radiation than on long-wave radiation. Reduced energy at the surface inhibits the formation of strong convection and leads to a stratiform type of cloud and rainfall. Later in the day (around 1400 LT), the convective rain is associated with vertical motions greater than  $3 \text{ ms}^{-1}$ , while those obtained in the stratiform clouds are an order of magnitude smaller. At higher altitude (6 km) the vertical motion is larger than  $8 \text{ ms}^{-1}$ , indicating very strong convective activity there.

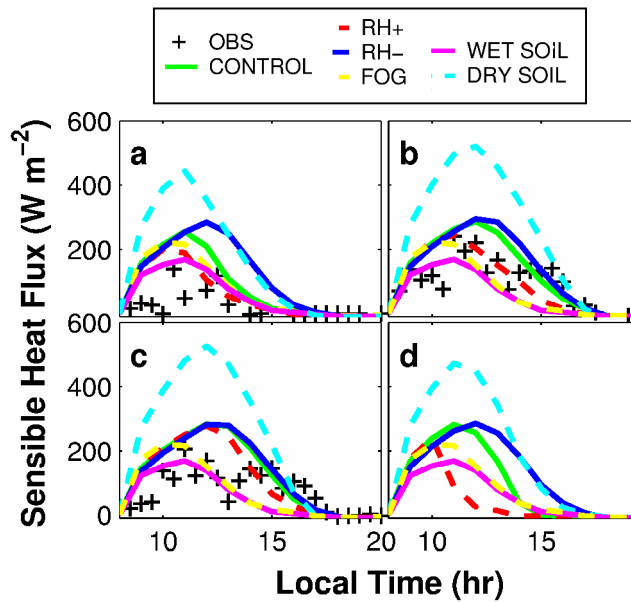


**FIG. 10.** Simulated domain-average sensible heat flux for the control and sensitivity experiments on (a) 04 February, (b) 06 February, (c) 14 February, and (d) 23 February. Black crosses represent available observations at (a) Jaru Forest, and (b)-(d) Ouro Preto D'Oeste.

As compared to dry soils, wet soils delay the onset of rainfall because the available energy at the ground surface is used primarily for evaporation, thus inhibiting the sensible heat that drives convection, as was already explained by Sud et al. (1993) and Betts et al. (1996). Rickenbach (2004) analyzed the diurnal formation of rain in the Amazon and found that occurrence of nocturnal rainfall delayed the next day convection. Our results are also supported by the work of Qian et al. (2004) who demonstrated that water recycling has an important effect on rainfall distribution. These results emphasize the complexity of the interactions taking place in the land-atmosphere system of this region, where water recycling is an important factor of its hydrometeorology (Eltahir 1996).

#### *d. Sensible and latent heat fluxes*

Formation of moist convection is highly dependent on the partition of energy at the ground surface (including vegetation) into sensible and latent heat fluxes. While the transfer of sensible heat between the surface and the atmosphere promotes the development of convective thermals, latent heat flux supplies the atmosphere with moisture. Figures 10 and 11 present the domain-average sensible and latent heat fluxes simulated with RAMS for all the control and sensitivity experiments performed in our study, together with observations.

In the first two hours of the simulations of the high- and low-atmospheric moisture experiments, heat fluxes are very similar to the control case. But after 1000 LT, a distinct pattern is noticed between the high- and low-initial atmospheric moisture simulations. In the high relative humidity case, clouds and rain cover larger areas as compared to the control and the dry atmospheric simulations. As a result, less solar radiation reaches the surface and both the sensible and latent heat fluxes are reduced (Figs. 10 and 11). Although less energy is available at the surface, large release of latent heat of condensation is produced during precipitation, thus maintaining convection. In the tropics, this release of heat is a major source of energy for the atmosphere. In the fog case, the sensible and latent heat fluxes are reduced as compared to the control simulations, reflecting the impact of cloudiness on the available radiative energy at the surface. It is interesting to note that a drier atmospheric profile, while producing less rainfall, allows the surface to release more latent heat in the atmosphere during the afternoon hours, thus increasing the atmospheric relative humidity that tends to increase rainfall. Thus, it has a negative feedback on the water recycling.

Soil moisture has a strong impact on the partition of energy absorbed at the surface into sensible and latent heat fluxes. Dry soils

cause a strong release of sensible heat and a weak release of latent heat (Figs. 10 and 11). This is due to the effects of the moisture stress on the vegetation, which close its stomata thus reducing (or even inhibiting in extreme cases) transpiration. The sensible heat peaks around 1200 LT, following the solar cycle. In this case, the low cloud-cover fraction allows more solar radiation to reach the surface. Wet soils result in low surface sensible heat and high latent heat fluxes. The lack of strong convection in that case is probably the main reason for the delayed rainfall, as illustrated in Figure 5.

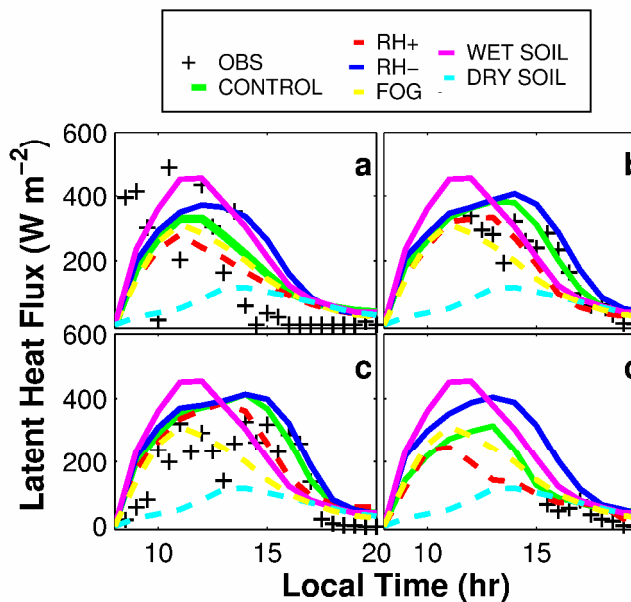


**FIG. 11.** Same as Fig. 10, but for the latent heat flux.

Heat and moisture fluxes were difficult to measure during the LBA/WetAMC campaign due to frequent rainfall. During rainy periods the eddy-correlation system often fails to provide reliable data. However, limited available observations indicate that simulations are comparable with observations at the towers. This is particularly well illustrated on the clearest day (F06) at Ouro Preto D'Oeste (Figs. 10b and 11b).

#### *e. Spatial variability*

Figures 12 and 13 depict the spatial distribution of accumulated precipitation for the cases of high- and low-moisture content in the atmosphere and the soil.

The low relative humidity experiments produce less rainfall accumulation and precipitation tends to occur mostly on the lee side of the mountains (Fig. 12a-d). This is mainly visible over the hills located in the northeastern part of the domain. High atmospheric humidity results not only in early and enhanced rainfall as illustrated in Fig. 5, but it also affects the location of its maximum accumulation (Fig. 12e-f). As compared to the rainfall obtained for the simulations initialized and forced with low relative humidity, precipitation is obtained earlier and at upwind locations. In general, the storms are advected by the predominant wind in the free atmosphere (illustrated by arrows in Fig. 12). Accordingly, rain accumulates in regions where the wind is coming from. Indeed, it rains more in the eastern part of the domain in those cases when easterly winds are dominant (F04, F06, and F14), and in the northwestern part of the domain on F23. In addition, precipitation spreads over larger areas as compared to the control run and the dry atmosphere case (Table 3).

Dry soils produce early convection and induce rainfall in the hills where thermals are better organized by the dynamical effects of topography (Gopalakrishnan et al. 2000) (Fig. 13a-d). On F14, the lack of moisture in the soil and the low atmospheric relative humidity produce light rainfall. But on F23 the combination of high sensible heat flux and atmospheric moisture produce strong convective cells. High soil moisture delays and shifts the rainfall accumulation downwind (Fig. 13e-h). High amounts of rainfall accumulate in the northwestern part of the domain on F04 and F14, and on the

lee side of the northeast mountains on F06 and F23. This also suggests that a better knowledge of initial soil-moisture conditions are likely to improve the simulations, as was shown in previous studies (Cheng and Cotton 2004; Weaver 2004).

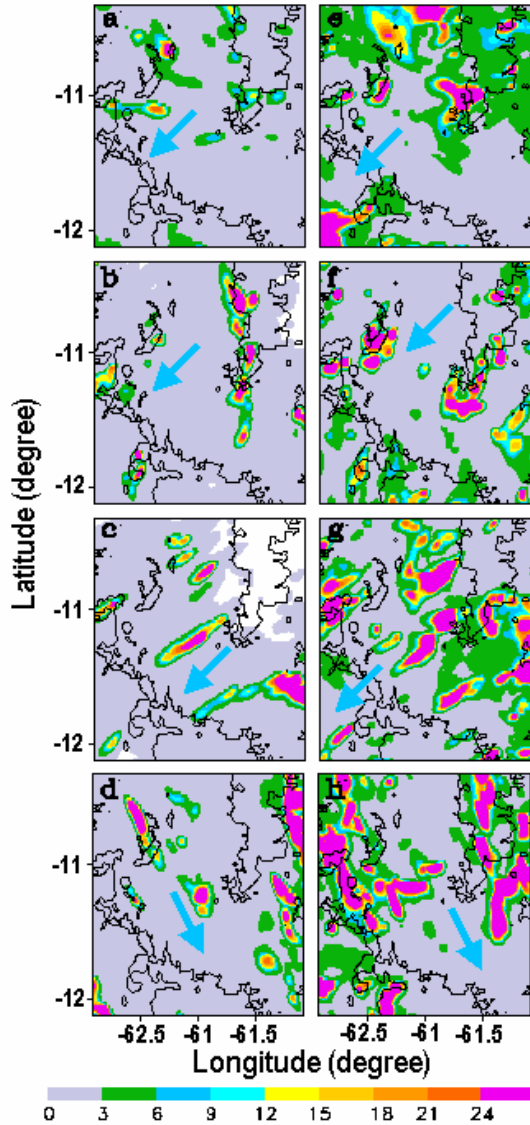


**FIG. 12.** Same as Fig. 4, but for low (left) and high (right) initial relative humidity on (a, e) 04 February, (b, f) 06 February, (c, g) 14 February, and (d, h) 23 February.

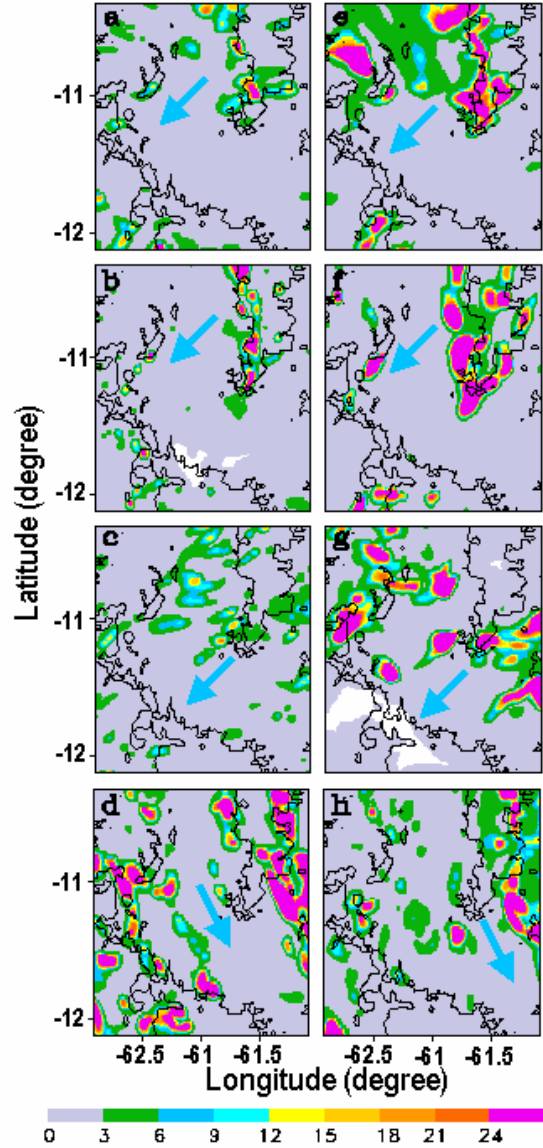


**FIG. 13.** Same as Fig. 12, but for low (left) and high (right) initial soil moisture.

#### *f. Sensitivity to grid size*

Previous numerical experiments conducted to simulate the hydrometeorology of the Amazon basin have used grid elements larger than 2 km (Silva Dias and Regnier 1996; Wang et al. 2000; Silva Dias et al. 2002). Here, we evaluate the impact of grid size on the model performance.

Figure 14 presents the domain-average, accumulated rainfall simulated with RAMS

set-up with different grid-element sizes as compared to the corresponding estimates derived from the S-POL radar. In general, coarser grids (i.e., 2 and 4 km) tend to produce less rainfall as compared to observations. However, on F14, high rainfall is produced in the center of the simulated domain (Fig. 15c), increasing the mean accumulation. In that case two factors affect precipitation there, the low initial relative humidity (see Fig. 2c) and the easterly winds in the entire atmosphere (see Fig. 7c). Early in the morning, the dry atmosphere inhibits cloud formation allowing solar radiation to reach the surface and to heat it. Also, the easterly winds transport the convective cells away from the mountains where they are generated towards the center of the domain.

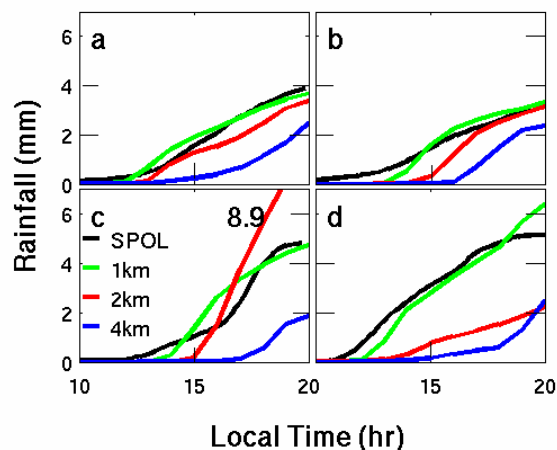


**FIG. 14.** Simulated domain-average accumulated rainfall with different numerical grid sizes on (a) 04 February, (b) 06 February, (c) 14 February, and (d) 23 February.

The same case simulated with a 4-km grid results in weaker and downstream rainfall accumulation. Coarser grids delay rainfall onset by about 3-4 hours. Additional simulations using grid elements of 20 km do not produce any rainfall accumulation (not shown). Weisman et al. (1997) and Salvador et al. (1999) also indicated that coarse-

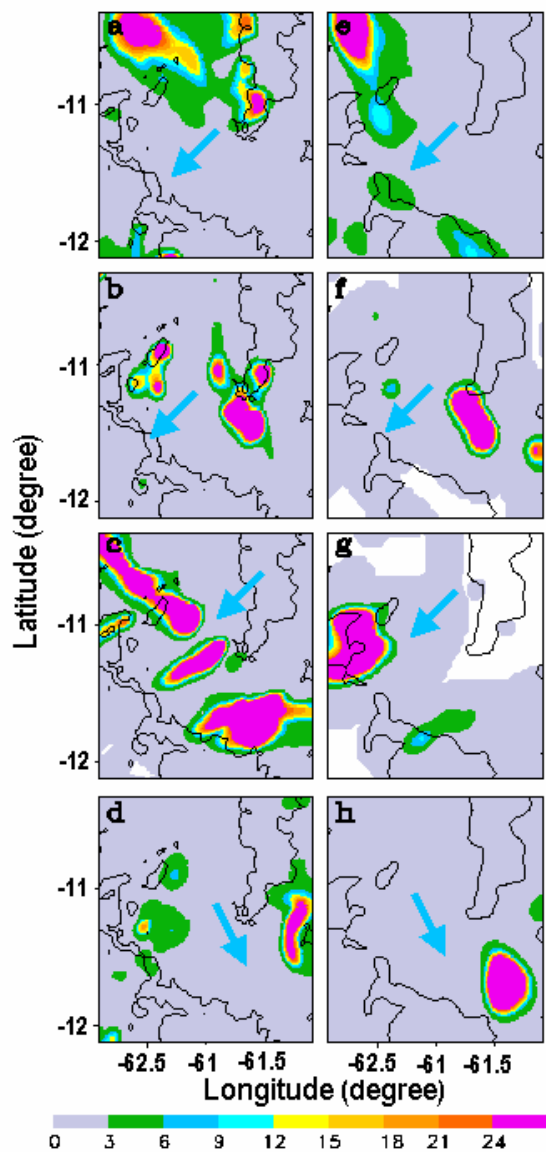
resolution simulations result in slower evolution of convective storms. They concluded that grid elements on the order of 2-4 km would be sufficient to resolve mid-latitude meteorological events. The sensitivity analysis performed here indicates that much better results are obtained with a grid whose elements are not larger than 1km.

Figure 15 displays the accumulated rainfall for the simulations using grid elements of 2 and 4 km. These “coarse-grid” simulations do not resolve some of the meso- $\gamma$  scale (i.e., 2-20 km) features captured with the S-POL radar and the high-resolution (control) simulations. Also, the slower evolution of convection produces rainfall accumulation more downstream as compared to the control simulation. As the grid-element size increases, less rainfall accumulates near the hills.

#### 4. Summary and conclusions

A series of numerical simulations were performed to evaluate the capability of the Regional Atmospheric Modeling System (RAMS) to simulate the evolution of convection in the Amazon basin during the rainy season and to elucidate some of the complex land-atmosphere interactions taking place in that region. Overall, we demonstrated that RAMS can simulate properly the domain-average accumulated rainfall in Rondônia, when reliable initial profiles of relative humidity and soil moisture are provided. An increase (decrease) of the initial relative humidity by only 10% generates significantly more (less) and earlier (delayed) rainfall. Other models, such as the operational ECMWF Integrated Forecast System (IFS), simulated too early rainfall in the wet season in Rondônia (Betts and Jakob 2002). In another study, Silva Dias et al. (2002) used RAMS to simulate a squall line that formed in February 1999 for the same region that was simulated here and noticed a delayed precipitation as compared

to observations. The tests performed here elucidate some of the factors that can affect quite significantly timing, rate and location of rainfall.



**FIG. 15.** Same as Fig. 12, but for grid sizes of 2 km (left) and 4 km (right).

The simulations described here emphasize that RAMS can provide a good estimate of the total area experiencing rainfall. But it is important to keep in mind that convection is chaotic in nature and, therefore, one cannot expect to obtain the exact same timing and location of a precipitation cell in the

observations and the model. Rather, the statistical properties of the rainfall pattern need to be duplicated by the model. It should also be mentioned that landscape features tend to anchor convective rain and the model does respond to this mechanism. Our sensitivity tests show that initial relative humidity and soil moisture affect the timing and spatial rainfall accumulation. In general, more water in the soil and/or the atmosphere produces more rainfall. But these conditions affect the onset of rainfall in opposite ways; while higher relative humidity leads to early rainfall, higher soil moisture delays its formation.

The impact of soil moisture content on the timing and rainfall location creates a negative feedback that works to homogenize the spatial distribution of rainfall and land water content. Indeed, a wet soil delays convection and produces more precipitation downstream. These results agree with previous simulations of theoretical landscapes, which show that convective rain developed over the dryer part of the landscape, creating a negative feedback (Chen and Avissar 1994; Avissar and Liu 1996; Emori 1998). This probably has significant ecological implications that it would be interesting to investigate with an appropriate vegetation dynamics model coupled to RAMS. We are currently in the process of developing such a coupled model.

Early morning atmospheric humidity appears to be quite important for the simulation of rainfall in this region. A nocturnal rainfall event raises the soil moisture and delays the onset of the next day convective rain. Otherwise, the moisture remains in the atmosphere and leads to earlier rainfall the next morning. Thus, models that are unable to represent nocturnal rainfall in the Amazon will likely fail to simulate rainfall due to misrepresentation of early morning atmospheric and soil moisture. The implications of these daily changes in timing and location for long-term

hydroclimate simulations of the Amazon remain to be studied.

The land-surface energy-budget partition into sensible and latent heat fluxes affects the amount of heat and moisture released into the atmosphere and, as a result, the vertical gradients and the atmospheric stability. This also affects whether clouds and precipitation will be convective or stratiform in nature. Convective cells grow deep, have strong upward motion, are more effective in creating rain, and allow more solar radiation to pass through their cloud-free downward branches, thus enhancing the radiative energy absorbed at the ground surface. By contrast, stratiform clouds are shallow but they cover larger areas and reduce the amount of solar radiation that reaches the surface, leading to light vertical motion and rain. The demonstrated capability of RAMS to simulate these two types of raining clouds is quite important because the land-cover change in this region may affect their relative distribution and, as a result, the local hydroclimate.

Sensitivity tests to model resolution show that a grid size of not more than 1 km is needed to simulate properly the averaged rainfall accumulation in this region. This is explained by the fact that large amounts of precipitation are produced by relatively small convective cells, which are neither parameterized nor explicitly resolved at grid-element sizes larger than 2 km.

Finally, the numerical experiments performed in this study indicate the existence of complex hydrometeorological feedback in the land-atmosphere system, involving atmospheric and soil moisture. To understand the hydroclimatological implications of these processes, it is necessary to perform long-term, high-resolution simulations, which require large computing resources. We are in the processes of performing such simulations

and will report our results in subsequent publications.

*Acknowledgments.* This research was supported by NASA under Grants NAG 5-8213 and NAG 5-9359, by the NSF under Grant ATM-0346554, and by the Gordon and Betty Moore Foundation. The views expressed herein are those of the authors and do not necessarily reflect the views of NASA, NSF or the Moore Foundation.

## REFERENCES

- Alvala, R. C. S., and Coauthors, 2002: Intradiurnal and seasonal variability of soil temperature, heat flux, soil moisture content, and thermal properties under forest and pasture in Rondonia. *J. Geophys. Res.*, **107**, doi:10.129/2001JD000599.
- Avissar, R., and R. A. Pielke, 1989: A parameterization of heterogeneous land surfaces for atmospheric numerical-models and its impact on regional meteorology. *Mon. Wea. Rev.*, **117**, 2113-2136.
- Avissar, R., and Y. Q. Liu, 1996: Three-dimensional numerical study of shallow convective clouds and precipitation induced by land surface forcing. *J. Geophys. Res.*, **101**, 7499-7518.
- Avissar, R., E. W. Eloranta, K. Gurer, and G. J. Tripoli, 1998: An evaluation of the large-eddy simulation option of the regional atmospheric modeling system in simulating a convective boundary layer: A FIFE case study. *J. Atmos. Sci.*, **55**, 1109-1130.
- Avissar, R., and C. A. Nobre, 2002: The Large-Scale Biosphere-Atmosphere Experiment in Amazonia (LBA). *J. Geophys. Res.*, **107**, doi:10.1029/2002JD002507.
- Avissar, R., P. L. Silva Dias, M. A. Silva Dias, and C. A. Nobre, 2002: The Large Scale Biosphere Atmosphere Experiment in Amazonia (LBA). Insights and future

- research needs. *J. Geophys. Res.*, **107**, doi:10.129/2002JD002704.
- Avissar, R., and D. Werth, 2005: Global hydroclimatological teleconnections resulting from tropical deforestation. *J. Hydrometeor.*, **6**, 134-145.
- Baidya Roy, S., and R. Avissar, 2002: Impact of land use/land cover change on regional hydrometeorology in Amazonia. *J. Geophys. Res.*, **107**, doi:10.129/2000JD000266.
- Beljaars, A. C. M., P. Viterbo, M. J. Miller, and A. K. Betts, 1993: The anomalous rainfall over the United States during July 1993: sensitivity to land surface parameterization and soil moisture anomalies. *Mon. Wea. Rev.*, **124**, 362-383.
- Betts, A., J. H. Ball, and J. Fuentes, 2002: Calibration and Correction of LBA/TRMM ABRACOS pasture site merged dataset. [Available online from <http://lba.cptec.inpe.br/>]
- Betts, A. K., J. H. Ball, A. C. M. Beljaars, M. J. Miller, and P. A. Viterbo, 1996: The land surface-atmosphere interaction: A review based on observational and global modeling perspectives. *J. Geophys. Res.*, **101**, 7209-7225.
- Betts, A. K., and C. Jakob, 2002: Evaluation of the diurnal cycle of precipitation, surface thermodynamics, and surface fluxes in the ECMWF model using LBA data. *J. Geophys. Res.*, **107**, doi:10.129/2001JD000427.
- Calvet, J. C., R. C. S. Alvala, G. Jaubert, C. Delire, C. Nobre, I. Wright, and J. Noilhan, 1997: Mapping surface parameters for mesoscale modeling in forested and deforested Southwestern Amazonia. *Bull. Amer. Meteor. Soc.*, **78**, 413-423.
- Carey, L. D., R. Cifelli, W. Petersen, and S. Rutledge, 2000: TRMM - LBA rainfall estimation using the S-POL radar. [Available online from [http://radarmet.atmos.colostate.edu/trmm\\_lba/spol\\_rain\\_info/PrelimRptLBASPOLrain.htm](http://radarmet.atmos.colostate.edu/trmm_lba/spol_rain_info/PrelimRptLBASPOLrain.htm).]
- Chang, J. T., and P. J. Wetzel, 1991: Effects of spatial variations of soil-moisture and vegetation on the evolution of a prestorm environment - a numerical case-study. *Mon. Wea. Rev.*, **119**, 1368-1390.
- Chen, F., and R. Avissar, 1994: The impact of land-surface wetness heterogeneity on mesoscale heat fluxes. *J. Appl. Meteor.*, **33**, 1323-1340.
- Cheng, W. Y. Y., and W. R. Cotton, 2004: Sensitivity of a cloud-resolving simulation of the genesis of a mesoscale convective system to horizontal heterogeneities in soil moisture initialization. *J. Hydrometeor.*, **5**, 934-958.
- Chou, S. C., A. M. B. Nunes, and I. F. A. Cavalcanti, 2000: Extended range forecasts over South America using the regional ETA model. *J. Geophys. Res.*, **105**, 10147-10160.
- Chou, S. C., C. A. S. Tanajura, Y. K. Xue, and C. A. Nobre, 2002: Validation of the coupled ETA/SSiB model over South America. *J. Geophys. Res.*, **107**, doi:10.129/2000JD000270.
- Cotton, W. R., and Coauthors, 2003: RAMS 2001: Current status and future directions. *Meteor. Atmos. Phys.*, **82**, 5-29.
- Cutrim, E., D. W. Martin, and R. Rabin, 1995: Enhancement of cumulus clouds over deforested lands in Amazonia. *Bull. Amer. Meteor. Soc.*, **76**, 1801-1805.
- Dawson, T. E., 1993: Hydraulic lift and water use by plants: Implications for water balance, performance, and plant-plant interactions. *Oecologia*, **95**, 565-574.
- Deardorff, J. W., 1980: Stratocumulus-capped mixed layers derived from a 3-dimensional model. *Bound.-Layer Meteor.*, **18**, 495-527.

- Druyan, L. M., M. Fulakeza, and P. Lonergan, 2002: Dynamic downscaling of seasonal climate predictions over Brazil. *J. Climate*, **15**, 3411-3426.
- Durieux, L., L. A. T. Machado, and H. Laurent, 2003: The impact of deforestation on cloud cover over the Amazon arc of deforestation. *Remote Sens. Environ.*, **86**, 132-140.
- Eltahir, E. A. B., 1996: Role of vegetation in sustaining large-scale atmospheric circulations in the tropics. *J. Geophys. Res.*, **101**, 4255-4268.
- Emanuel, K. A., 1994: *Atmospheric Convection*. Oxford University Press Inc., 580 pp.
- Emori, S., 1998: The interaction of cumulus convection with soil moisture distribution: An idealized simulation. *J. Geophys. Res.*, **103**, 8873-8884.
- Gandu, A. W., J. C. P. Cohen, and J. R. S. Souza, 2004: Simulation of deforestation in eastern Amazonia using a high-resolution model. *Theor. Appl. Climatol.*, **78**, 123-135.
- Gash, J. H. C., and C. A. Nobre, 1997: Climatic effects of Amazonian deforestation: Some results from ABRACOS. *Bull. Am. Meteor. Soc.*, **78**, 823-830.
- Gopalakrishnan, S. G., S. B. Roy, and R. Avissar, 2000: An evaluation of the scale at which topographical features affect the convective boundary layer using large eddy simulations. *J. Atmos. Sci.*, **57**, 334-351.
- Goulding, M., R. Barthem, and E. J. G. Ferreira, 2003: *The Smithsonian Atlas of the Amazon*. Smithsonian Books, 253 pp.
- Halverson, J. B., T. Rickenbach, B. Roy, H. Pierce, and E. Williams, 2002: Environmental characteristics of convective systems during TRMM-LBA. *Mon. Wea. Rev.*, **130**, 1493-1509.
- Harrington, J. Y., 1997: The effects of radiative and microphysical processes on simulated warm and transition season arctic stratus., Atmospheric Department, Colorado State University, 288 pp.
- Hasler, N., R. Avissar, and G. E. Liston, 2005: Issues in simulating the annual precipitation of a semi-arid region in Central Spain. *J. Hydrometeor.*, **6**, 409-422.
- Henderson-Sellers, A., K. McGuffie, and H. Zhang, 2002: Stable isotopes as validation tools for global climate model predictions of the impact of Amazonian deforestation. *J. Climate*, **15**, 2664-2677.
- Henderson-Sellers, A., and A. J. Pitman, 2002: Comments on "Suppressing impacts of the Amazonian deforestation by the global circulation change". *Bull. Amer. Meteor. Soc.*, **83**, 1657-1661.
- Horel, J. D., J. B. Pechmann, A. N. Hahmann, and J. E. Geisler, 1994: Simulations of the Amazon Basin circulation with a regional model. *J. Climate*, **7**, 56-71.
- INPE, 2002: Monitoring the Brazilian Amazon gross deforestation. [Available online from [http://www.grid.inpe.br/amz/prodes2000/html/pag\\_2.htm](http://www.grid.inpe.br/amz/prodes2000/html/pag_2.htm).]
- Kalnay, E., and Coauthors, 1996: The NCEP/NCAR 40-year reanalysis project. *Bull. Amer. Meteor. Soc.*, **77**, 437-471.
- Klemp, J. B., and R. B. Wilhelmson, 1978: The simulation of three-dimensional convective storm dynamics. *J. Atmos. Sci.*, **35**, 1070-1096.
- Laurent, H., L. A. T. Machado, C. A. Morales, and L. Durieux, 2002: Characteristics of the Amazonian mesoscale convective systems observed from satellite and radar during the WETAMC/LBA experiment. *J. Geophys. Res.*, **107**, doi:10.1029/2001JD000338.
- Liston, G. E., and R. A. Pielke, 2001: A climate version of the regional atmospheric modeling system. *Theor. Appl. Climatol.*, **68**, 155-173.

- Lorenz, E. N., 1963: Deterministic non-periodic flow. *J. Atmos. Sci.*, **20**, 131-140.
- Louis, J. F., 1979: Parametric model of vertical eddy fluxes in the atmosphere. *Bound.-Layer Meteor.*, **17**, 187-202.
- Mellor, G. L., and T. Yamada, 1974: A hierarchy of turbulence closure models for planetary boundary layers. *J. Atmos. Sci.*, **31**, 1791-1806.
- Meyers, M. P., R. L. Walko, J. Y. Harrington, and W. R. Cotton, 1997: New RAMS cloud microphysics parameterization .2. The two-moment scheme. *Atmos. Res.*, **45**, 3-39.
- Misra, V., P. A. Dirmeyer, B. P. Kirtman, H. M. H. Juang, and M. Kanamitsu, 2002: Regional simulation of interannual variability over South America. *J. Geophys. Res.*, **107**, doi:10.129/2001JD900216.
- Molinari, J., and M. Dudek, 1992: Parameterization of convective precipitation in mesoscale numerical models: A critical review. *Mon. Wea. Rev.*, **120**, 326-344.
- Nair, U. S., R. O. Lawton, R. M. Welch, and R. A. Pielke, 2003: Impact of land use on Costa Rican tropical montane cloud forests: Sensitivity of cumulus cloud field characteristics to lowland deforestation. *J. Geophys. Res.*, **108**, doi:10.129/2001JD001135.
- NCAR, 1999: SPOL TRMM-LBA Brazil 1999. [Available online from <http://www.atd.ucar.edu>.]
- Negri, A. J., R. F. Adler, L. M. Xu, and J. Surratt, 2004: The impact of Amazonian deforestation on dry season rainfall. *J. Climate*, **17**, 1306-1319.
- Nepstad, D. C., and Coauthors, 1994: The role of deep roots in the hydrological and carbon cycles of Amazonian forests and pastures. *Nature*, **372**, 666-669.
- Nobre, C. A., P. J. Sellers, and J. Shukla, 1991: Amazonian deforestation and regional climate change. *J. Climate*, **4**, 957-988.
- Pielke, R. A., and Coauthors, 1992: A comprehensive meteorological modeling system - RAMS. *Meteor. Atmos. Phys.*, **49**, 69-91.
- Pielke, R. A., T. J. Lee, J. H. Copeland, J. L. Eastman, C. L. Ziegler, and C. A. Finley, 1997: Use of USGS-provided data to improve weather and climate simulations. *Ecol. Appl.*, **7**, 3-21.
- Qian, J. H., W. K. Tao, and K. M. Lau, 2004: Mechanisms for torrential rain associated with the Mei-Yu Development during SCSMEX 1998. *Mon. Wea. Rev.*, **132**, 3-27.
- Rao, V. B., I. F. A. Cavalcanti, and K. Hada, 1996: Annual variation of rainfall over Brazil and water vapor characteristics over South America. *J. Geophys. Res.*, **101**, 26539-26551.
- Richey, J. E., R. L. Victoria, E. Salati, and B. R. Forsberg, 1991: The biogeochemistry of a major river system: The Amazon case study. *Biogeochemistry of Major World Rivers*, J. E. Richey, Ed., John Wiley & Sons, 57-74.
- Rickenbach, T. M., 2004: Nocturnal cloud systems and the diurnal variation of clouds and rainfall in southwestern Amazonia. *Mon. Wea. Rev.*, **132**, 1201-1219.
- Roads, J., and Coauthors, 2003: International Research Institute/Applied Research Centers (IRI/ARCs) regional model intercomparison over South America. *J. Geophys. Res.*, **108**, doi:10.1029/2002JD003201.
- Salvador, R., J. Calbo, and M. M. Millan, 1999: Horizontal grid size selection and its influence on mesoscale model simulations. *J. Appl. Meteor.*, **38**, 1311-1329.
- Silva Dias, M. A., and P. Regnier, 1996: Simulation of mesoscale circulations in a deforested area of Rondonia in the dry

- season. *Amazonian Deforestation and Climate*, R. L. Victoria, Ed., J. Wiley & Sons, 531-547.
- Silva Dias, M. A., and Coauthors, 2002: A case study of convective organization into precipitating lines in the Southwest Amazon during the WETAMC and TRMM-LBA. *J. Geophys. Res.*, **107**, doi:10.129/2001JD000375.
- Souza, E. P., N. O. Renno, and M. A. Silva Dias, 2000: Convective circulations induced by surface heterogeneities. *J. Atmos. Sci.*, **57**, 2915-2922.
- Sud, Y. C., W. C. Chao, and G. K. Walker, 1993: Dependence of rainfall on vegetation - Theoretical considerations, simulation experiments, observations, and inferences from simulated atmospheric soundings. *J. Arid. Environ.*, **25**, 5-18.
- Take, E. S., and Coauthors, 1999: Project to Intercompare Regional Climate Simulations (PIRCS): Description and initial results. *J. Geophys. Res.*, **104**, 19443-19461.
- Tanajura, C. A. S., 1996: Modeling and analysis of the South American summer climate, Department of Meteorology, University of Maryland, 164 pp.
- Vital, H., and K. Stattegger, 2000: Sediment dynamics in the lowermost Amazon. *J. Coastal Res.*, **16**, 316-328.
- Walko, R. L., W. R. Cotton, M. P. Meyers, and J. Y. Harrington, 1995: New Rams cloud microphysics parameterization .1. The single-moment scheme. *Atmos. Res.*, **38**, 29-62.
- Walko, R. L., and Coauthors, 2000a: Coupled atmosphere-biophysics-hydrology models for environmental modeling. *J. Appl. Meteor.*, **39**, 931-944.
- Walko, R. L., W. R. Cotton, G. Feingold, and B. Stevens, 2000b: Efficient computation of vapor and heat diffusion between hydrometeors in a numerical model. *Atmos. Res.*, **53**, 171-183.
- Wang, J. F., R. L. Bras, and E. A. B. Eltahir, 2000: The impact of observed deforestation on the mesoscale distribution of rainfall and clouds in Amazonia. *J. Hydrometeor.*, **1**, 267-286.
- Weaver, C. P., and R. Avissar, 2001: Atmospheric disturbances caused by human modification of the landscape. *Bull. Amer. Meteor. Soc.*, **82**, 269-281.
- Weaver, C. P., 2004: Coupling between large-scale atmospheric processes and mesoscale land-atmosphere interactions in the U.S. Southern Great Plains during summer. Part I: case studies. *J. Hydrometeor.*, **5**, 1223-1246.
- Weisman, M. L., and J. B. Klemp, 1986: Characteristics of isolated convective storms. *Mesoscale Meteorology and Forecasting*, P. S. Ray, Ed., American Meteorological Society, 793.
- Weisman, M. L., W. C. Skamarock, and J. B. Klemp, 1997: The resolution dependence of explicitly modeled convective systems. *Mon. Wea. Rev.*, **125**, 527-548.
- Werth, D., and R. Avissar, 2002: The local and global effects of Amazon deforestation. *J. Geophys. Res.*, **107**, doi:10.129/2001JD000717.

This document was created with Win2PDF available at <http://www.win2pdf.com>.  
The unregistered version of Win2PDF is for evaluation or non-commercial use only.